

## Supporting Information

### **Achieving efficient inverted perovskite solar cells with excellent electron transport and stability by employing ladder-conjugated perylene diimide dimer**

Helin Wang,<sup>ab</sup> Fu Yang,<sup>c</sup> Yuren Xiang,<sup>b</sup> Shuai Ye,<sup>b</sup> Xiao Peng,<sup>b</sup> Jun Song,<sup>\*b</sup> Junle  
Qu,<sup>b</sup> Wai-Yeung Wong<sup>\*a</sup>

<sup>a</sup> Department of Applied Biology and Chemical Technology, The Hong Kong Polytechnic University, Hung Hom, Hong Kong, P. R. China

<sup>b</sup> Key Laboratory of Optoelectronic Devices and Systems of Ministry of Education and Guangdong Province, College of Physics and Optoelectronic Engineering, Shenzhen University, Shenzhen 518060, P. R. China.

<sup>c</sup> Institute of Materials for Electronics and Energy Technology (i-MEET), Department of Materials Science and Engineering, Friedrich-Alexander-Universität Erlangen-Nürnberg, Martensstrasse 7, 91058 Erlangen, Germany.

## 1. Materials and Characterization

IDTT was purchased from Derthon Optoelectronic Materials Co., CH<sub>3</sub>NH<sub>3</sub>I (MAI) and Br-PDI were synthesized using previously reported methods in the literature.<sup>[16,17]</sup> PbI<sub>2</sub> (99.999%) was purchased from Alfa Aesar. PMMA and F4-TCNQ were purchased from Xi'an Polymer Light Technology Corp. (China). PTAA was purchased from 1-Material (Canada). [6,6]-Phenyl-C<sub>61</sub>-butyric acid methyl ester (PCBM) and 4,7-diphenyl-1,10-phenanthroline (Bphen) were purchased from Nichem Fine Technology Co. Ltd. (Taiwan). N,N-dimethylformamide (DMF, 99.5%), dimethylsulfoxide (DMSO, 99.5%), 2-butanol (99.5%), chlorobenzene (99.5%), ethyl acetate (99.5%) and ethanol (99.5%) were purchased from Sigma Aldrich. 3,4,9,10-Perylenetetracarboxylic dianhydride, tris(dibenzylideneacetone)dipalladium and tris(2-methylphenyl) phosphine were purchased from Aladdin (China). The indium-tin-oxide (ITO) on glass was purchased from Xiangcheng Science and Technology Co. Ltd. Other commercially available reagents were purchased from TCI Chemical Co. and used without further purification unless otherwise stated. Solvents for chemical reactions were purified according to the standard procedures. All chemical reactions were carried out under an inert atmosphere.

<sup>1</sup>H and <sup>13</sup>C NMR spectra were recorded using a 400 MHz Bruker NMR spectrometer in CDCl<sub>3</sub> at 293 K using TMS as a reference. The accurate mass correction was measured with matrix-assisted laser desorption-ionization time-of-flight (MALDI-TOF) mass spectrometer (MALDI micro MX). UV-Vis spectra were measured with the UV-Vis spectrophotometer (Model HP8453) in a 1 cm quartz cell. Cyclic voltammetry (CV) were recorded on a BSA100B/W electrochemical workstation using glassy carbon discs as the working electrode, Pt wire as the counter electrode and Hg/Hg<sub>2</sub>Cl<sub>2</sub> electrode as the reference electrode. 0.05 M tetrabutylammonium hexafluorophosphate (Bu<sub>4</sub>NPF<sub>6</sub>) dissolved in dichloromethane was employed as the supporting electrolyte, which was calibrated by the ferrocene/ferroncenium (Fc/Fc<sup>+</sup>) as the redox couple. The energy level of Fc/Fc<sup>+</sup> is 5.08 eV relative to vacuum. Thermogravimetric analysis (TGA) was carried out using

a Mettler Toledo TGA/SDTA 851e at a heating rate of 10 °C min<sup>-1</sup> under the nitrogen flow of 20 mL min<sup>-1</sup>.

## 2. Device fabrication and measurement

Device Fabrication: The 5 wt% F4-TCNQ doped PTAA precursor solution (5 mg mL<sup>-1</sup>) was prepared by dissolving PTAA and F4-TCNQ in chlorobenzene. The PMMA precursor solution (0.5 mg mL<sup>-1</sup>) was prepared by dissolving PMMA in ethyl acetate. The MAPbI<sub>3</sub> precursor solution was prepared by dissolving 1.037 g PbI<sub>2</sub> and 0.376 g MAI (PbI<sub>2</sub>:MAI molar ratio = 1:1.05) into 1.35 mL DMF and 0.15 mL DMSO mixed solvent. The IDTT2FPDI precursor solutions of different concentrations were prepared by dissolving IDTT2FPDI in chlorobenzene. The 10 mg mL<sup>-1</sup> PCBM precursor solution was prepared by dissolving PCBM in chlorobenzene. The 0.7 mg mL<sup>-1</sup> Bphen precursor solution was prepared by dissolving Bphen in ethanol.

The perovskite solar cells were fabricated as follows. First, the indium tin oxide (ITO) substrates (2×2 cm<sup>2</sup>) were ultrasonically and subsequently cleaned with deionized water, acetone, and isopropanol for 15 min, respectively. Then, the substrates were dried by blowing nitrogen and then treated with O<sub>3</sub> plasma for 15 min before use. After that, a PTAA:F4-TCNQ precursor solution was spin-coated on the cleaned ITO at 6000 revolutions per minute (rpm) for 20 s. Then, the films were annealed at 100 °C on a hot plate for 2 min. For the deposition of the thin passivation layer, the PMMA precursor solution was spin-coated on the top of the ITO/PTAA:F4-TCNQ substrates at 6000 rpm for 20 s, and then annealed at 100 °C for 2 min. After the substrates were cooled down, the MAPbI<sub>3</sub> precursor solution was spin-coated on the ITO/PTAA:F4-TCNQ/PMMA substrates at 6000 rpm for 20 s. 300 μL 2-butanol was used as the anti-solvent and was dropped on the wet MAPbI<sub>3</sub> precursor film at the 8 s during the spin-coating process, and then the films were annealed at 100 °C for 10 s. The above spin-coating processes were conducted in a glove box under a nitrogen atmosphere and with a real-time humidity of <1 ppm. Finally, the perovskite films were transferred on a hot plate, first annealed in ambient air (at 100 °C, for 15 min,

with a real-time humidity of 55–65%), and then annealed under the DMSO atmosphere with the same temperature and time. For the DMSO atmosphere, 100  $\mu\text{L}$  DMSO was dropped into a small ceramic crucible, and then a glass Petri dish was used to cover the samples and crucible. After the films were cooled down, the IDTT2FPDI precursor solution (10 mg  $\text{mL}^{-1}$ ) was spin-coated on the perovskite layer at 2500 rpm for 30 s, and the PCBM precursor solution was spin-coated on the IDTT2FPDI layer at 2500 rpm for 30 s. Then, the Bphen precursor solution was spin-coated without additional annealing. The devices were completed by evaporating a 100 nm thick aluminum film as the electrode. The active device area was set as 0.12  $\text{cm}^2$  ( $0.3 \times 0.4 \text{ cm}^2$ ) by the overlapping area between the top Al cathode and the bottom ITO anode.

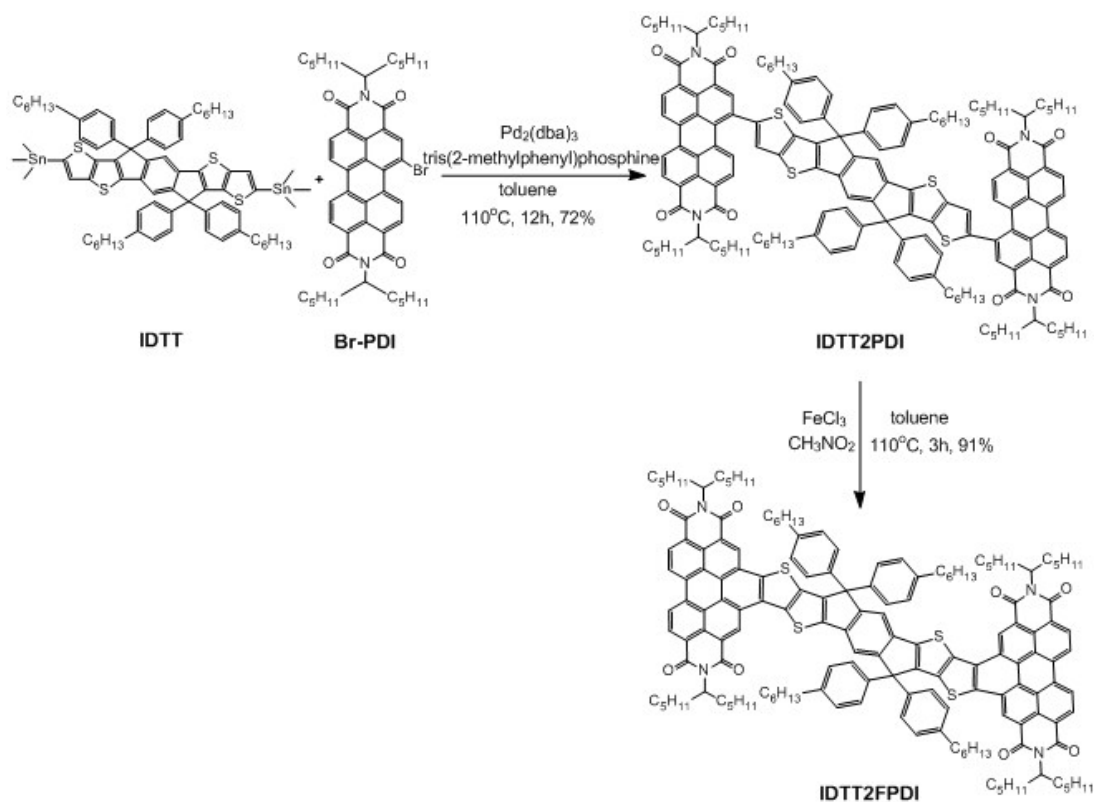
The electron-only devices for PCBM or IDTT2FPDI films were fabricated as follows. The 1.5 M ZnO precursor solution was spin-coated on the cleaned ITO at 4000 rpm for 30 s and then annealed at 200  $^{\circ}\text{C}$  for 30 min. After the films were cooled down, the PCBM or IDTT2FPDI chlorobenzene solution (20 mg  $\text{mL}^{-1}$ ) was spin-coated at 1000 rpm for 30 s without additional annealing. Finally, Ca (10 nm) and Al (100 nm) films were evaporated on top of the active layer as the electrode.

The electron-only devices for perovskite films were fabricated as follows. The 0.5 M  $\text{SnO}_2$  precursor solution was spin-coated on the cleaned ITO at 2000 rpm for 30 s and then annealed at 150  $^{\circ}\text{C}$  for 30 min. The rest of the fabrication steps is similar to the fabrication of PSCs.

Device Characterization: SEM images were obtained with a Zeiss Supra 55 microscope. AFM images were obtained from Bruker Dimension Icon AFM. A sun simulator (Zolix Sirius-SS) was used to provide the simulated solar irradiation (AM 1.5G, 100  $\text{mW cm}^{-2}$ ).  $J$ - $V$  characteristics were measured using a Keithley 2400 source meter. The output of the light source was adjusted using a calibrated silicon photodiode (ABET technology). The  $J$ - $V$  curves were measured by forward scan from -0.5 to 1.5 V and reverse scan from 1.5 to -0.5 V. The EQE was measured using a power source (Zolix Sirius-SS) with a monochromator (Zolix Omni- $\lambda$ ) and a source meter (Keithley 2400). The stability of the PSCs was kept in the dark condition at

room temperature and under controlled humidity of about 25% room humidity (RH). The samples were taken out to be tested in the forward scan rate of 0.1 V/s after every 12 hours. The FLIM measurements and TRPL decay traces were measured by a Leica TCS SP8 system using the TCSPC technique with laser excitation at 600 nm and detection at 770 nm. The steady-state PL spectra were measured by the fluorescence spectrophotometer (OmniPL-microS, Zolix, China), a 600 nm continuous wave laser came into the films from the air side. Water contact angles were measured by the contact angle instrument (SZ-CAMD33, China).

### 3. Synthesis



Scheme S1. Synthetic route of IDTT2FPDI.

IDTT2PDI: Br-PDI (0.2 g, 0.26 mmol), IDTT (0.15 g, 0.11 mmol),  $\text{Pd}_2(\text{dba})_3$  (24 mg, 0.026 mmol) and tris(2-methylphenyl)phosphine (32 mg, 0.10 mmol) were added to 10 mL dry toluene and the mixture was stirred at  $110^\circ\text{C}$  under an argon

atmosphere. After 12 hours, the solvent was stripped off by a rotary evaporator, and the crude product was purified by silica gel column chromatography with petroleum ether:dichloromethane (1:1, v/v) as eluent to give IDTT2PDI (72%, 0.19 g, 0.08 mmol). <sup>1</sup>H NMR (400 MHz, CDCl<sub>3</sub>, 25 °C) : δ (ppm) = 8.76-8.56 (m, 10H, Ar H), 8.38-8.31 (m, 2H, Ar H), 8.29-8.19 (m, 2H, Ar H), 7.63 (s, 2H, Ar H), 7.54 (s, 2H, Ar H), 7.18-7.16 (d, 8H, Ar H), 7.11-7.09 (d, 8H, Ar H), 5.21-5.13 (m, 4H, CH), 2.65-2.51 (m, 8H, CH<sub>2</sub>), 2.31-2.16 (m, 8H, CH<sub>2</sub>), 1.93-1.78 (m, 8H, CH<sub>2</sub>), 1.66-1.53 (m, 8H, CH<sub>2</sub>), 1.42-1.21 (m, 72H, CH<sub>2</sub>), 0.90-0.78 (m, 36H, CH<sub>3</sub>).

IDTT2FPDI: IDTT2PDI (0.3 g, 0.12 mmol) was added to 15 mL dry toluene and the solution was stirred at room temperature under an argon atmosphere. Then a solution of ferric chloride (0.5 g, 3.11 mmol) in nitromethane (0.7 mL) was added to the reaction solution, and the mixture was stirred at 110 °C for 3 hours. After this mixture was cooled to room temperature and poured into the mixed solvents of dichloromethane (50 mL) and water (50 mL), the organic layer was separated and extracted three times with dichloromethane, and dried over magnesium sulfate. The solvent was stripped off by a rotary evaporator, and the crude product was purified by silica gel column chromatography with petroleum ether:dichloromethane (3:2, v/v) as eluent to afford IDTT2FPDI (91%, 0.27 g, 0.11 mmol). <sup>1</sup>H NMR (400 MHz, CDCl<sub>3</sub>, 25 °C) : δ (ppm) = 9.86-9.80 (d, 1H, Ar H), 9.44 (s, 1H, Ar H), 9.11-8.88 (m, 8H, Ar H), 7.94 (s, 4H, Ar H), 7.50-7.48 (d, 8H, Ar H), 7.34-7.32 (d, 8H, Ar H), 5.35-5.32 (m, 4H, CH<sub>2</sub>), 2.70-2.66 (t, 8H, CH<sub>2</sub>), 2.39-2.37 (m, 8H, CH<sub>2</sub>), 2.04-2.01 (m, 8H, CH<sub>2</sub>), 1.70-1.67 (m, 8H, CH<sub>2</sub>), 1.37-1.25 (m, 72H, CH<sub>2</sub>), 0.89-0.84 (m, 36H, CH<sub>3</sub>); <sup>13</sup>C NMR (100 MHz, CDCl<sub>3</sub>, 25 °C) : δ (ppm) = 165.04, 146.51, 142.43, 139.56, 138.54, 137.94, 137.81, 137.45, 135.94, 135.70, 134.83, 132.87, 129.06, 128.16, 125.80, 125.15, 122.95, 121.93, 54.44, 35.74, 32.50, 31.89, 31.37, 29.71, 29.20, 26.93, 26.80, 22.67, 22.59, 14.13, 11.01; MALDI-TOF-MS: calculated for C<sub>160</sub>H<sub>174</sub>N<sub>4</sub>O<sub>8</sub>S<sub>4</sub>, 2407.2215 [M+Na]<sup>+</sup>, found 2430.2254.

#### 4. Supporting tables and figures

**Table S1.** Device performance of perovskite solar cells with different IDTT2FPDI film thickness.

Thickness	$J_{sc}$ [mA cm <sup>-2</sup> ]	$V_{oc}$ [V]	$FF$ [%]	$PCE$ [%]
0	22.0	1.09	71.4	17.1
8	23.8	1.09	72.8	18.9
14	23.9	1.10	73.8	19.4
19	23.7	1.10	72.6	19.0
24	23.7	1.10	72.7	18.9
28	23.8	1.10	72.2	18.8
32	23.4	1.10	72.7	18.8

**Table S2.** Device performance of conventional perovskite solar cells with or without IDTT2FPDI as an ETL.

ETL	Scan direction	$J_{sc}$ [mA cm <sup>-2</sup> ]	$V_{oc}$ [V]	$FF$ [%]	$PCE$ [%]
SnO <sub>2</sub> /IDTT2FPDI	Forward scan	23.8	1.09	72.3	18.7
SnO <sub>2</sub> /IDTT2FPDI	Reverse scan	23.8	1.09	71.9	18.7
SnO <sub>2</sub>	Forward scan	22.1	1.09	72.8	17.6
SnO <sub>2</sub>	Reverse scan	23.1	1.09	68.7	17.3

**Table S3.** Device performance of perovskite solar cells with IDTT2FPDI as single ETL.

ETL	Scan direction	$J_{sc}$ [mA cm <sup>-2</sup> ]	$V_{oc}$ [V]	$FF$ [%]	$PCE$ [%]
IDTT2FPDI	Forward scan	20.6	1.10	72.1	16.3
IDTT2FPDI	Reverse scan	20.5	1.10	71.7	16.1

**Table S4.** Device performance of perovskite solar cells with different PDI-based ETL in the literature and this work.

Perovskite	ETL	Structure	$V_{oc}$ [V]	$J_{sc}$ [mA cm <sup>-2</sup> ]	$FF$ [%]	$PCE$ [%]	Ref.
MAPbI <sub>3</sub>	FPDI	conventional	1.08	19.8	38.5	8.25	21
MAPbI <sub>3</sub>	PDI-EH	invert	0.83	19.7	61.0	10.3	22
CS <sub>0.05</sub> FA <sub>0.81</sub> MA <sub>0.14</sub> PbI <sub>2.55</sub> Br <sub>0.45</sub>	TiO <sub>2</sub> /TCI-PDI	conventional	1.07	17.9	76.8	14.7	23
MAPbI <sub>3</sub>	di-PDI-DMBI/TiO <sub>2</sub>	invert	0.86	21.6	54.0	10.0	24
MAPbI <sub>2.5</sub> Br <sub>0.5</sub>	PDI/C60	invert	0.93	19.3	61.4	11.0	25
MAPbI <sub>3</sub> (Cl)	TiO <sub>2</sub> /PPDI-F3N	conventional	1.09	22.8	73.7	18.3	26
MAPbI <sub>3</sub>	Br-PDI/ZnO	invert	0.83	18.9	66.9	10.5	27
MAPbI <sub>3-x</sub> Br <sub>x</sub>	PPDIDTT/PCBM	invert	0.99	21.1	79.1	16.5	28
MAPbI <sub>3-x</sub> Cl <sub>x</sub>	N-PDI	conventional	1.08	21.8	75.0	17.7	29
MAPbI <sub>3</sub>	TiO <sub>2</sub> /PDI2	conventional	1.07	23.0	78.9	19.8	30
MAPbI <sub>3</sub>	TPE-PDI <sub>4</sub> /C60	invert	1.05	22.0	81.0	18.8	31
MAPbI <sub>3</sub>	PDI-C <sub>60</sub>	invert	1.06	22.1	79.2	18.6	32
MAPbI <sub>3</sub>	PV-PDI	invert	0.93	16.6	65.6	10.1	33
<b>MAPbI<sub>3</sub></b>	<b>IDTT2FPDI/PCBM</b>	<b>invert</b>	<b>1.10</b>	<b>23.9</b>	<b>73.8</b>	<b>19.4</b>	<b>this work</b>

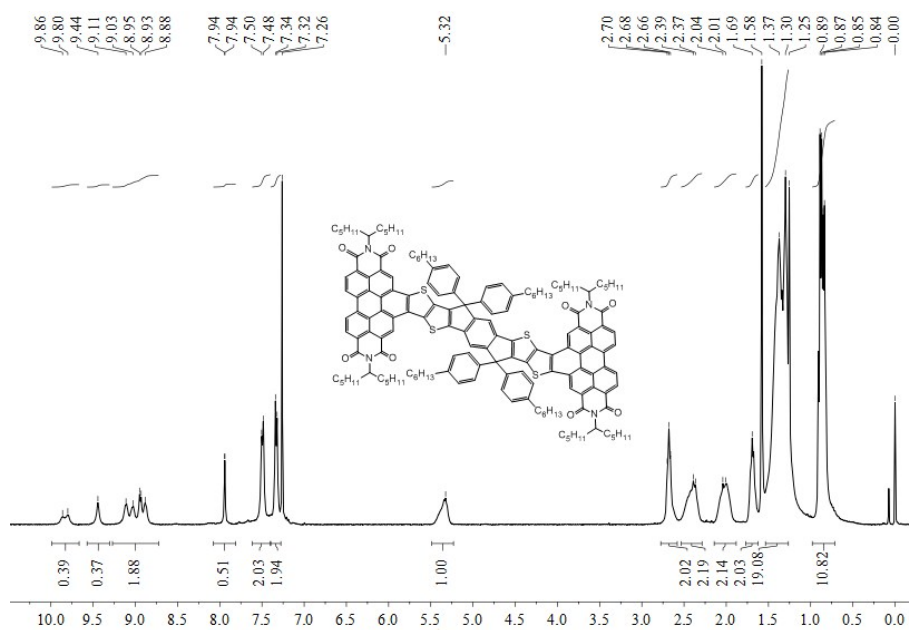


**Figure S1.** <sup>1</sup>H NMR spectrum of IDTT2FPDI in CDCl<sub>3</sub>.



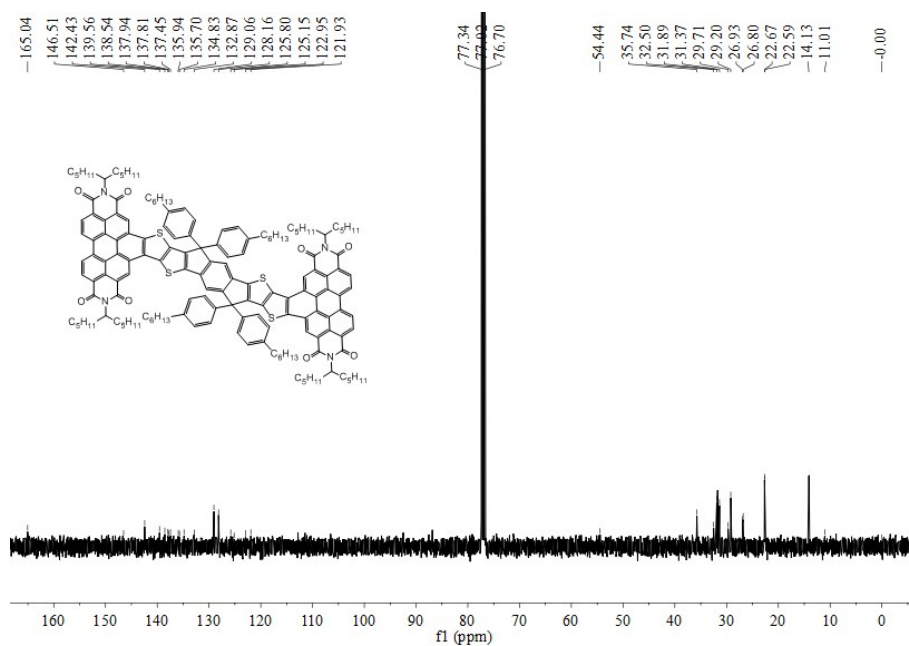


**Figure S2.**  $^{13}\text{C}$  NMR spectrum of IDTT2FPDI in  $\text{CDCl}_3$ .

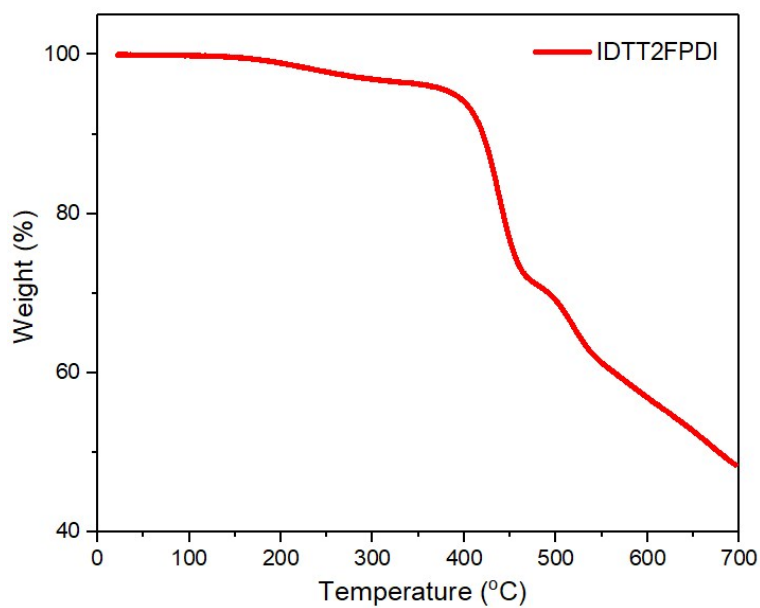


**Figure S3.** Thermogravimetric analysis plot of IDTT2FPDI.

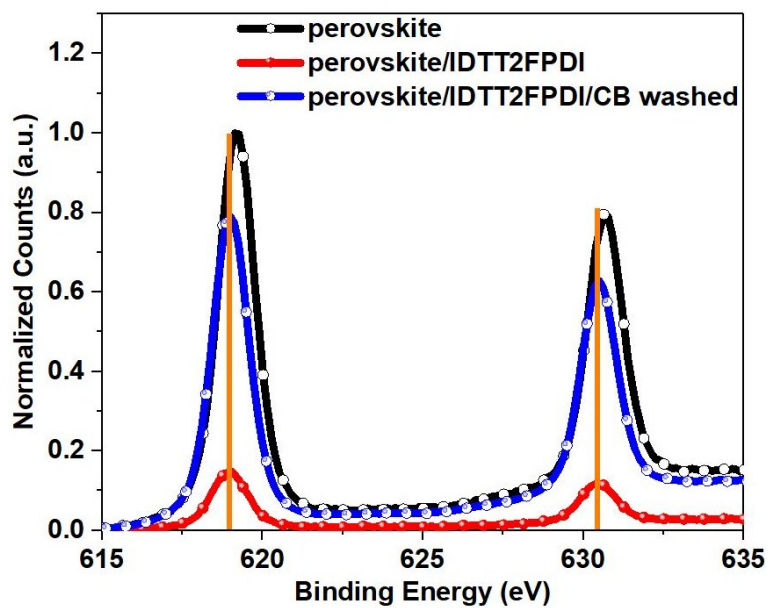


**Figure S4.** XPS core level spectra of I 3d for pure perovskite film and two IDTT2FPDI-covered perovskite films.

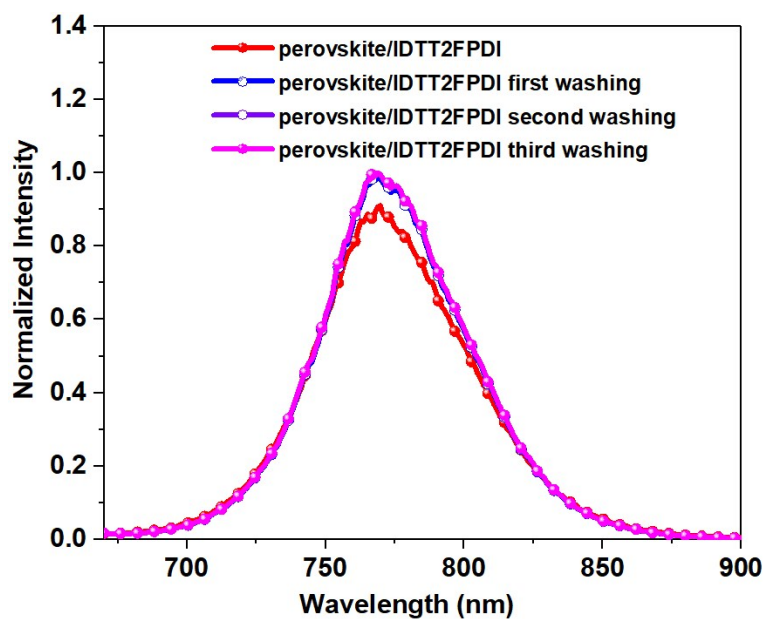


**Figure S5.** Steady-state PL spectra for IDTT2FPDI-covered perovskite films with a different number of washing.

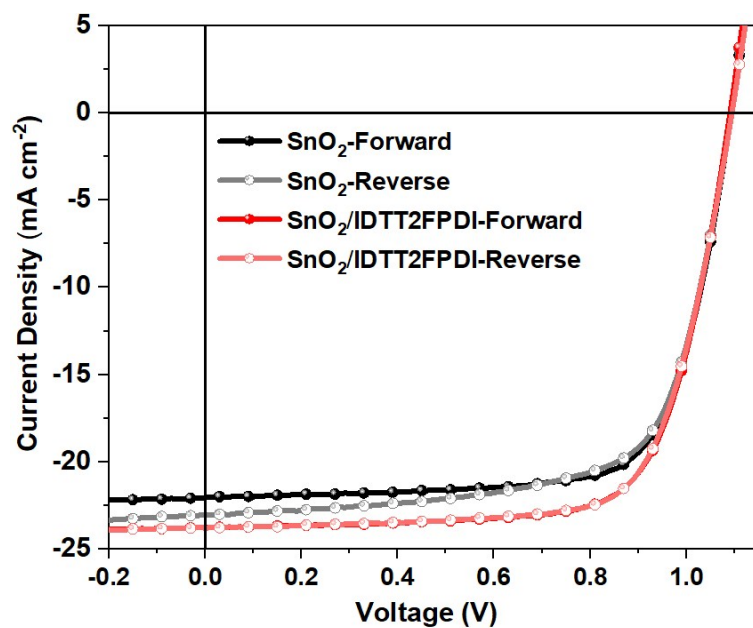


**Figure S6.** Forward and reverse scanning of the conventional perovskite solar cells using SnO<sub>2</sub> or SnO<sub>2</sub>/IDTT2FPDI as the ETL, respectively.

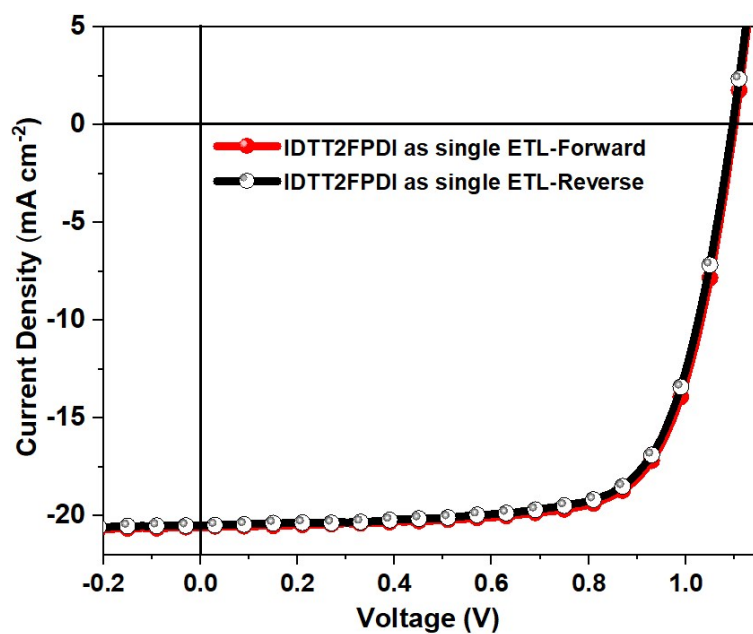


**Figure S7.** Forward and reverse scanning of the inverted perovskite solar cells using IDTT2FPDI as single ETL.